Monitoring-Based Fatigue Reliability Assessment of Steel Bridges: Analytical Model and Application

Y. Q. Ni, M.ASCE[1]; X. W. Ye[2]; and J. M. Ko, F.ASCE[3]

Abstract: A fatigue reliability model which integrates the probability distribution of hot spot stress range with a continuous probabilistic formulation of Miner's damage cumulative rule is developed for fatigue life and reliability evaluation of steel bridges with long-term monitoring data. By considering both the nominal stress obtained by measurements and the corresponding stress concentration factor (SCF) as random variables, a probabilistic model of the hot spot stress is formulated with the use of the *S-N* curve and the Miner's rule, which is then used to evaluate the fatigue life and failure probability with the aid of structural reliability theory. The proposed method is illustrated using the long-term strain monitoring data from the instrumented Tsing Ma Bridge. A standard daily stress spectrum accounting for highway traffic, railway traffic, and typhoon effects is derived by use of the monitoring data. Then global and local finite element models (FEMs) of the bridge are developed for numerically calculating the SCFs at fatigue-susceptible locations, while the stochastic characteristics of SCF for a typical welded T-joint are obtained by full-scale model experiments of a railway beam section of the bridge. A multimodal probability density function (PDF) of the stress range is derived from the monitoring data using the finite mixed Weibull distributions in conjunction with a hybrid parameter estimation algorithm. The failure probability and reliability index versus fatigue life are achieved from the obtained joint PDF of the hot spot stress in terms of the nominal stress and SCF random variables.

Introduction

Fatigue is a progressive and localized process in which structural damage accumulates continuously due to the repetitive application of external loadings such as vehicles for steel bridges; while these applied loadings may be well below the structural resistance capacity. In a pervasive perspective of metal fatigue, the fatigue process is deemed to initiate from an internal or surface flaw where the stresses are concentrated, and originally consists of shear flow along slip planes. Suffering from an amount of load cycles, this slip generates intrusions and extrusions and ultimately results in forming into a crack. With the propagation of cracks, it will eventually lead to fatigue failure in the structural components (Schijve 2001). Fatigue is one of the main causes involved in fatal mechanical failures of civil engineering structures as well as transportation facilities and infrastructure systems. Such devastat-

ing events occur suddenly and result in heavy losses of life and property (Reed et al. 1983; Fisher 1984; Stephens et al. 2001). Among the current fatigue analysis methodologies, the nominal stress-life (*S-N*) approach has widely been used for fatigue-related design and evaluation of aircraft, offshore structures, and steel bridges (Schilling et al. 1978; Moses et al. 1987; Mohammadi et al. 1998; Connor and Fisher 2006; Albrecht and Lenwari 2009). When the nominal stress-life approach stipulated in specifications is adopted for bridge fatigue damage and life evaluation, it is necessary to know the stress spectra of welded details in critical locations and the *S-N* curves of the details. The stress spectra can be acquired from a theoretical stress analysis by assuming a traffic loading model and a structural model. However, their accuracy may be very limited due to the errors in both loading and structural modeling. The consequence of inaccurate estimation of the stress spectra would be significant in view of the fact that the predicted fatigue life is inversely proportional to at least the cube of the stress range (Gurney 1979).

Recent advances in sensing, data acquisition, computing, communication, data and information management, have greatly promoted the applications of structural health monitoring (SHM) technology in bridge structures. On-line SHM systems play a vital role in continuously providing huge amounts of monitoring data for reliably assessing the integrity, durability, and reliability of bridges (DeWolf et al. 2002; Pines and Aktan 2002; Wong 2004; Ko and Ni 2005; Brownjohn 2007). The measurement data of dynamic strain/stress is of great value in achieving the authentic field-based stress spectra for conducting fatigue evaluation of steel bridges. Due to the limitation of sensor implementation techniques and specific in situ conditions, however, the sensors for

[1]Professor, Dept. of Civil and Structural Engineering, Hong Kong Polytechnic Univ., Hung Hom, Kowloon, Hong Kong (corresponding author). E-mail: ceyqni@polyu.edu.hk

[2]Ph.D. Candidate and Research Associate, Dept. of Civil and Structural Engineering, Hong Kong Polytechnic Univ., Hung Hom, Kowloon, Hong Kong.

[3]Chair Professor, Dept. of Civil and Structural Engineering, Hong Kong Polytechnic Univ., Hung Hom, Kowloon, Hong Kong.

strain monitoring usually are not deployed at the most critical locations where fatigue cracks are expected to occur and thus only the nominal strain/stress is obtained. To handle such a critical problem, the hot spot stress approach has been well accepted and recommended by several national and international codes and standards [European Committee for Standardization (CEN) 1992; American Welding Society (AWS) 1998; International Institute of Welding (IIW) 2000]. This method takes into account the dimensions and stress-concentrating effects, in which the nominal stress is transformed into the value of structural stress at the hot spot by multiplying an SCF.

Research efforts have been devoted by a number of investigators for determining the SCFs of various structural joints and assessing the fatigue condition of structural components by means of hot spot stress. Gandhi and Berge (1998) conducted fatigue tests on seven different T-joints made of circular brace and rectangular chord in constant amplitude axial loading and compared the SCF measured experimentally with various existent parametric formulas. Morgan and Lee (1998a,b) carried out an extensive parametric study of the distribution of SCF for the in-plane moment loading and out-of-plane moment loading case in tubular K-joints commonly found in offshore platforms and proposed a new equation to determine SCF on the chord and the brace. Doerk et al. (2003) explained and compared various procedures for evaluating structural hot spot stress at different types of welded joints. Chiew et al. (2004) and Lie et al. (2004) investigated experimentally and numerically the fatigue performance of cracked tubular T-joint subjected to in-plane bending only, a combination of in-plane bending and out-of-plane bending, and a combination of axial loading, in-plane bending and out-of-plane bending, respectively. Poutiainen et al. (2004) investigated the limits and accuracy of different methods for hot spot stress determination and compared them with finite-element analysis results from simple two-dimensional and precise three-dimensional models. Chan et al. (2005) reported that the hot spot stress approach gave a more appropriate fatigue life prediction than the nominal stress approach for a steel bridge.

In recognition of uncertainty and randomness inherent in the nature of fatigue phenomenon and test/measurement data, it is appropriate to conduct S-N curve-based fatigue life assessment in a probabilistic way as: (1) the number of fatigue test data for derivation of the S-N curves of specific structural joints is limited, and the data are subjected to pronounced statistical scatter; (2) there are significant disparities when using the stress-life experimental results of a specimen for component-level fatigue life assessment of real structures due to the difference of fatigue features between the test specimen and real structural components; and (3) the material characteristics as well as the stress history and environment exhibit uncertainty not only in the experimental process of fatigue test, but also during the service life of the real structure. In view of the above facts, investigations for probabilistic assessment of fatigue life have been carried out and most of them have focused on the usage of the S-N curve procedure (Crespo-Minguillon and Casas 1998; Szerszen et al. 1999; Cho et al. 2001; Kim et al. 2001; Pourzeynali and Datta 2005). Only a very limited amount of research is available on monitoring-based fatigue reliability assessment. The lack of such studies is mainly due to the challenging nature that a continuous monitoring process for compiling external load and structural response data and updating the structural performance against fatigue is costly and may not be easily applicable or economically viable for all types of structures (Mohammadi 2001; Ni et al. 2006).

A probabilistic method for fatigue evaluation of highway and railway bridges generally consists of: (1) the development of a stress distribution model from field monitoring data or by simulation; (2) the use of the Miner's rule (Miner 1945) for fatigue damage analysis along with an appropriate S-N relationship; and (3) the use of a probability function to describe the fatigue reliability of critical structural components. A comprehensive literature review on the existing fatigue reliability approaches for reassessment of steel structures, including railway and highway bridges, is available in Byers et al. (1997a,b). While the stress distribution function is not easily formulated due to the scatter of the data, a common theoretical distribution model is usually assumed. Also, the incorporation of SCF in fatigue reliability modeling for probabilistic fatigue life assessment has scarcely been addressed.

In the present study, a fatigue reliability model which integrates the probability distribution of hot spot stress range with a continuous probabilistic formulation of the Miner's damage cumulative rule is proposed to facilitate fatigue life and reliability evaluation of steel bridges using long-term monitoring data. By considering both the measurement-obtained nominal stress and the SCF as random variables, a probabilistic model of the hot spot stress is formulated for evaluating the fatigue life and the probability of failure. A hybrid parameter estimation algorithm is applied to formulate a multimodal PDF of the stress range from measurement data. The proposed procedure is illustrated using the long-term monitoring data of dynamic strain from the instrumented Tsing Ma Bridge.

Analytical Model and Treatment of Uncertainties

Fatigue Reliability Model

The classical method for predicting fatigue life is based on the S-N relationship or S-N curve. The S-N curve, obtained by cycling test specimens at constant amplitude stress, plots the fatigue life or number of cycles to failure, N, as a function of the stress range, S, and is represented by the following relationship (Basquin 1910):

$$NS^m = C \tag{1}$$

where C=constant for a given material and fatigue category and the exponent m=material parameter typically ranging between 2 and 4 (Byers et al. 1997a).

For variable amplitude stress cycles, the fatigue damage, D, can be evaluated by the Miner's rule (Miner 1945)

$$D = \sum_{i=1}^{n} \frac{n_i}{N_i} = \frac{n_1}{N_1} + \frac{n_2}{N_2} \cdots + \frac{n_n}{N_n} \tag{2}$$

where n_i=number of stress cycles for the ith stress range and N_i=number of stress cycles to failure in the structural component if the stress range is S_i. Usually, failure is assumed to occur when the damage measured $D=1$.

The nominal stress range, S, is represented by an algebraic difference between the maximum stress, σ_{max}, and the minimum stress, σ_{min}, measured in one stress cycle, and the hot spot stress range, S_h, is evaluated by multiplying the nominal stress range by an SCF. That is

$$S = \sigma_{max} - \sigma_{min} \tag{3}$$

$$S_h = S \times \mathrm{SCF} = (\sigma_{\max} - \sigma_{\min}) \times \mathrm{SCF} \qquad (4)$$

In the present study, the hot spot stress range is regarded as a function of two random variables: S and SCF. Upon the assumption that the two random variables are independent, the joint PDF of the hot spot stress range, $f(h)$, can be obtained as

$$f(h) = f(s) \times f(t) \qquad (5)$$

where $f(s)$ and $f(t)$=PDFs of the nominal stress range and the SCF, respectively.

When the joint PDF of the hot spot stress range is a continuous function, the Miner's rule given in Eq. (2) can be rewritten as the following expression to evaluate the fatigue damage characterized by a total of n_{tot} stress cycles:

$$D = \int \int_H \frac{n_{\mathrm{tot}} f(h)}{N_f} dh = \int_S \int_T \frac{n_{\mathrm{tot}} f(s) f(t)}{N_f} ds dt \qquad (6)$$

where N_f=stress cycles at failure.

Thus the fatigue life, F, can be expressed as

$$F = \frac{D_f}{D} = \frac{D_f}{\displaystyle\int_S \int_T \frac{n_{\mathrm{tot}} f(s) f(t)}{N_f} ds dt} \qquad (7)$$

in which

$$n_{\mathrm{tot}} = \sum_{i=1}^{n} \lambda_i n_i \qquad (8)$$

$$\lambda_i = \begin{cases} (S_i/S_0)^2 & \text{if } S_i < S_0 \\ 1 & \text{if } S_i > S_0 \end{cases} \qquad (9)$$

where λ_i=reducing factor; S_0=constant amplitude nonpropagating stress range; and D_f=fatigue damage at failure.

Then the limit-state (LS) function for fatigue damage can be expressed as

$$g(s,t) = D_f - \int_S \int_T \frac{n_{\mathrm{tot}} f(s) f(t)}{N_f} ds dt \qquad (10)$$

The probability of failure, p_f, and the reliability index, β, can be obtained by structural reliability theory as follows:

$$p_f = P\{g(s,t) \le 0\} = P\left\{ D_f - \int_S \int_T \frac{n_{\mathrm{tot}} f(s) f(t)}{N_f} ds dt \le 0 \right\} \qquad (11)$$

$$\beta = -\Phi^{-1}(p_f) \qquad (12)$$

where $\Phi(\bullet)$=standard normal cumulative distribution function (CDF).

Obviously, one of the key issues and challenges involved in the usage of the above fatigue reliability model for monitoring-based probabilistic fatigue life assessment is the exploration of probability distributions for both the stress range and SCF. The explicit modeling of these two probability distributions will be addressed in the following sections.

Uncertainty of Stress Range

The rainflow cycle counting method has a fundamental physical characteristic of its compatibility with the corresponding stress-strain relation by simply extracting stress amplitudes and cycles

in the stress time history associated with closed hysteresis loops (Downing and Socie 1982). The stress range of a structural component under stochastic load conditions can be performed using the rainflow counting algorithm only when the recorded stress time history is long enough (Nagode and Fajdiga 2006). When relatively short stress time histories are exclusively available, it is necessary to model the distribution of the stress range in the rainflow domain with a continuous PDF in order to adequately represent the stochastic stress states and extrapolate to the region which was not covered by the measured data. In this study, the treatment of uncertainty of the stress range is accomplished by making use of the finite mixture distributions in conjunction with a hybrid parameter estimation approach developed by Nagode and Fajdiga (1998).

Finite Mixture Distributions

The finite mixture distributions are commonly employed for modeling complex probability distributions and enable the statistical modeling of random variables with multimodal behavior where a simple parametric model fails to depict the characteristics of the observations adequately. The basic structure of finite mixture distributions for independent scalar or vector observations y can be written as (McLachlan and Peel 2000)

$$f(y|c,w,\boldsymbol{\theta}) = \sum_{l=1}^{c} w_l f_l(y|\boldsymbol{\theta}_l) \qquad (13)$$

$$\sum_{l=1}^{c} w_l = 1 \quad \text{and} \quad w_l \ge 0 \qquad (14)$$

where $f(y|c,w,\boldsymbol{\theta})$=predictive mixture density and $f_l(y|\boldsymbol{\theta}_l)$ =given parametric family of predictive component densities indexed by the scalar or vector parameters $\boldsymbol{\theta}_l$. The objective of the analysis is inference about the unknowns which include the number of components or groups, c, the component weights, w_l, summing to 1, and the component parameters, $\boldsymbol{\theta}_l$.

Thus, for instance, the finite mixed normal distributions and the finite mixed Weibull distributions can be expressed, respectively, by

$$f(y|c,w,\boldsymbol{\theta}) = \sum_{l=1}^{c} w_l \frac{1}{\sqrt{2\pi}} \exp\left\{ -\frac{1}{2} \frac{(y-\mu_l)^2}{\sigma_l^2} \right\} \qquad (15)$$

$$f(y|c,w,\boldsymbol{\theta}) = \sum_{l=1}^{c} w_l \frac{\gamma_l}{\theta_l} \left(\frac{y}{\theta_l}\right)^{\gamma_l-1} \exp\left\{ -\left(\frac{y}{\theta_l}\right)^{\gamma_l} \right\} \qquad (16)$$

where μ_l and σ_l=mean value and standard deviation of normal mixture parameters and γ_l and θ_l=Weibull shape parameters.

Hybrid Parameter Estimation

From an algorithmic point of view, the mixture problem can be formulated as an incomplete data problem (Steiner and Hudec 2007), and the identification of the mixture parameters as a latent variable problem is generally based on the well known expectation maximization algorithm albeit other methods are available (Titterington et al. 1985). In this study, a hybrid parameter estimation approach (Nagode and Fajdiga 2006) is used for estimation of the parameters of the finite mixture distributions. It is applicable for an arbitrary set of observations from an unknown number of classes and different parametric families. In this method, the preprocessing of observations can be accomplished either by the histogram, Parzen window or k-nearest neighbor
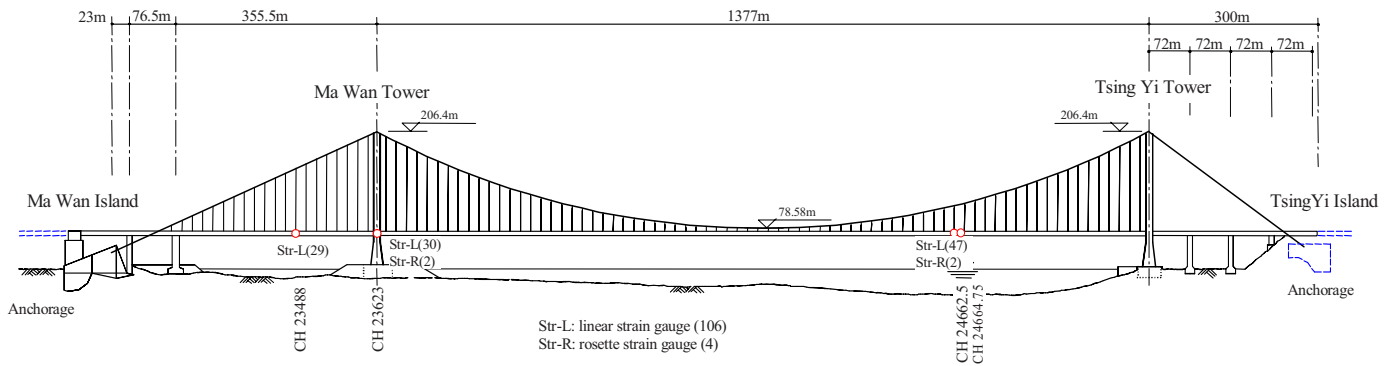
Fig. 1. Layout of strain gauges on Tsing Ma Bridge

approach, and the predictive component densities can be alternatively picked out of normal, lognormal, and Weibull parametric families. Moreover, the optimal number of components, weights, and component parameters can be gained iteratively by using the Akaike information criterion (AIC) (Akaike 1974).

The synopsis of the hybrid parameter estimation method is illustrated in Nagode and Fajdiga (2006). First, the set of independent scalar or vector observations is counted into a finite number of bins and meanwhile empirical densities are calculated. Then component weights and component parameters are estimated. This process consists of rough and enhanced component parameter estimation and the separation of observations, which is repeated until the discrepancy between the densities is beyond an acceptable limit. Thus the convergence of the predictive component density to the empirical one is the theoretical ground for the validation of the procedure. Subsequently, residual frequencies are distributed between the components by the Bayes decision rule (Duda and Hart 1973). Finally, optimal AIC is searched for iteratively, where optimal number of components, optimal weights, and optimal component parameters always coincide with minimal AIC.

Uncertainty of SCF

The SCF can be calculated by dividing the hot spot stress, σ_{hot}, by the nominal stress, σ_{nom}, according to

$$SCF = \frac{\sigma_{hot}}{\sigma_{nom}} \tag{17}$$

The hot spot stress, resulting from the local stress concentrations due to geometric irregularities and discontinuities at welded connections, is difficult to determine due to the extremely complicated stress distribution in the vicinity of the weld toe. It is commonly obtained by numerical finite element methods or experimental measurements using strain gauges (Niemi et al. 2006). When the finite-element method is used to conduct the hot spot stress analysis of a complex structure, a two-step procedure is suggested to be followed: (1) a global structural FEM is first established for conducting global structural analysis to determine the fatigue-critical zones and locations and (2) refined local FEMs of the desired critical regions are then constructed and analyzed to obtain the corresponding hot spot stress which can be determined directly at the location of the weld toe or through an extrapolation of the stresses at adjacent reference points. On the other hand, when tests are performed and strain measurements are used to determine the hot spot stress, an elaborate and reasonable instrumentation scheme of strain gauges is crucial. The experimental

determination of the structural hot spot stress is usually accomplished by extrapolation or regression of the stress distribution outside of the weld to the weld toe.

Steel bridges are usually composed of lots of longitudinal and transverse plate-type structural members with welded joints at their intersections, thus it is difficult to calculate the nominal stresses for the structural components of steel bridges in comparison with the structures mainly composed of bars or beams. When a bridge is instrumented with an online SHM system, this problem can be easily handled since the monitoring strain/stress data can be directly used as the nominal strain/stress for fatigue damage and life evaluation of the adjacent welded details.

Upon the achievement of the hot spot stress at the weld toe and the nominal stress at the location of the field-installed strain gauge, the SCF can then be obtained as the ratio of the hot spot stress to the nominal stress. Moreover, the SCF should be regarded as a random variable primarily due to the stochastic behavior of the loading conditions. However, so far scant attention has been paid to the investigation of statistical properties and probability distribution of the SCF. Alternatively, it is presumed to be a random variable with an assumed probability distribution. In the present study, the determination of the SCF and the identification of its probability distribution are achieved by use of the finite element method and full-scale model experiments. The full-scale model experiments of typical welded connections for stochastic characterization of the SCF are detailed in Ye (2010).

Illustration Using Field Monitoring Data

Monitoring Data of Dynamic Strain

The Tsing Ma Bridge in Hong Kong, as shown in Fig. 1, is a suspension bridge with a main span of 1,377 m carrying both highway and railway traffic. It forms a key part of the most essential transportation network linking the Hong Kong International Airport to the urban areas. After its construction in 1997, the bridge has been instrumented with a long-term SHM system comprising 283 sensors permanently installed on the bridge (Wong 2004; Wong and Ni 2009). As part of this monitoring system, 110 weldable foil-type strain gauges have been installed to measure dynamic strains at deck cross sections and bearings as shown in Fig. 1. Most of the strain gauges were attached to the fatigue-prone portions which were identified during the design of the SHM system.

One-year (the year of 1999) monitoring data from all the 110 strain gauges have been acquired for strain-based fatigue and con-
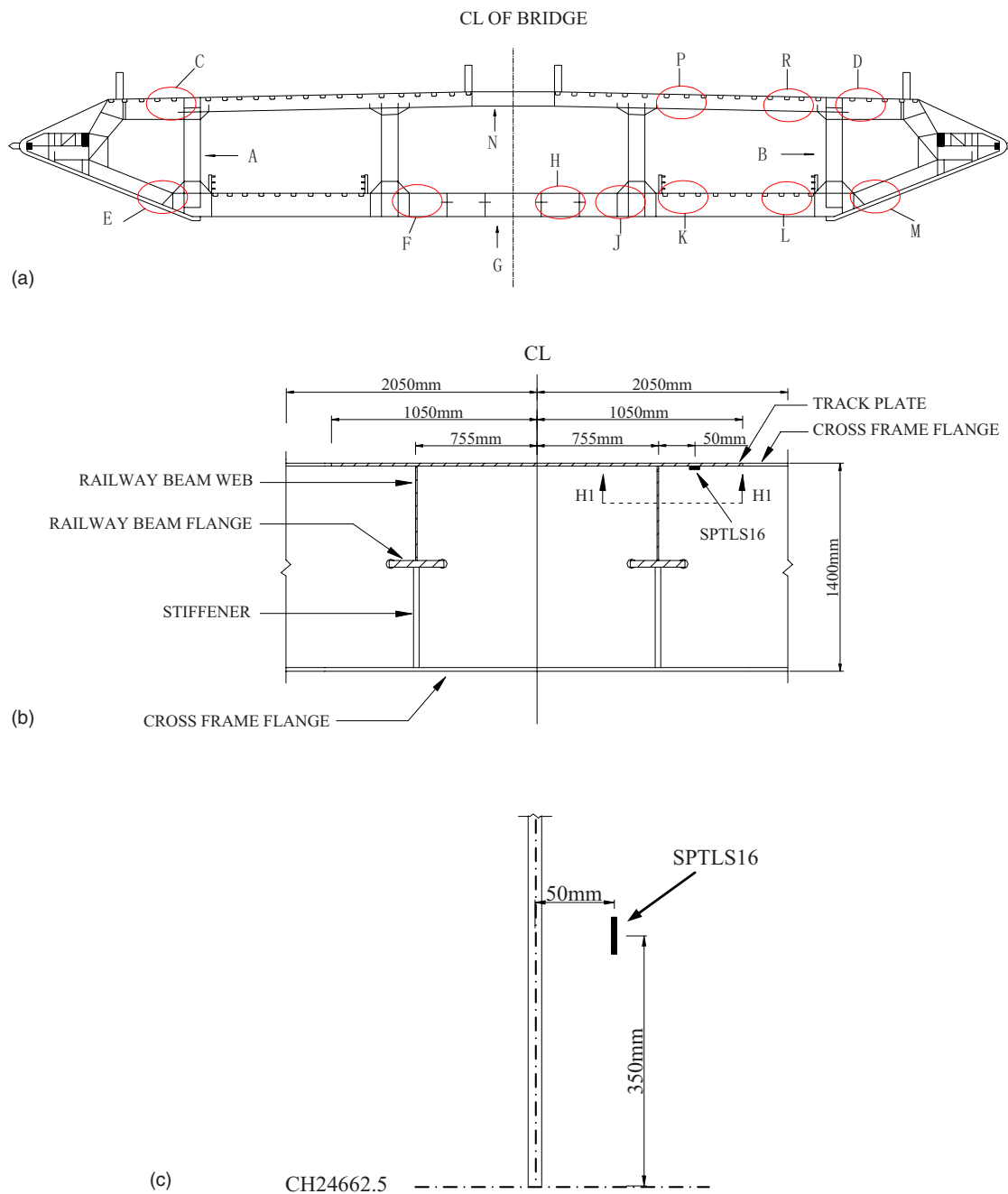
Fig. 2. Location of strain gauge SPTLS16 on deck cross section CH24662.5: (a) deck cross section CH24662.5; (b) sectional view of Detail H; and (c) section H1-H1

dition assessment. Presented in this paper are the results using the monitoring data from the strain gauge SPTLS16 located at the deck cross section CH24662.5 as illustrated in Fig. 2. The strain gauge SPTLS16 was installed under the track plate of the railway beam composed of two inverted T-beams welded to the top flange plate, denoted as Detail H in Fig. 2(a). Figs. 2(b and c) show the sectional view of Detail H.

The strain data were recorded continuously at a sample frequency of 51.2 Hz. Fig. 3 illustrates two typical daily strain time histories obtained from the strain gauge SPTLS16. By examining the measured data, the following observations are made: (1) the daily strain-time curves exhibit some common characteristics in the shape of curve and magnitude of cycles, and there are almost no strain pulses from 1:30 a.m. to 5:30 a.m. since the airport

railway ceases its daily service during this period; (2) many strain pulses with large amplitudes are observed in each daily strain time history, which are the strain responses caused by train traffic; and (3) the overall drift of the strain-time curve is significant, which is attributed to the environmental factors such as temperature and solar radiation. This drift does not influence the calculation of stress range since the stress range depends only on the difference between the peak and the valley of each stress cycle, as defined in Eq. (3).

Stress Spectrum

The stress time history is obtained through simply multiplying the measured strain data by the elastic modulus of steel. After seeking
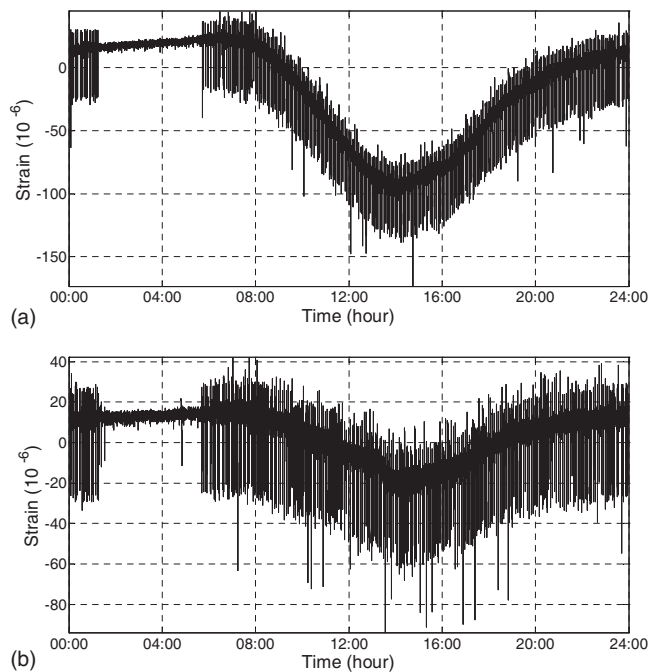
Fig. 3. Measured daily strain time histories: (a) September 23, 1999; (b) November 6, 1999

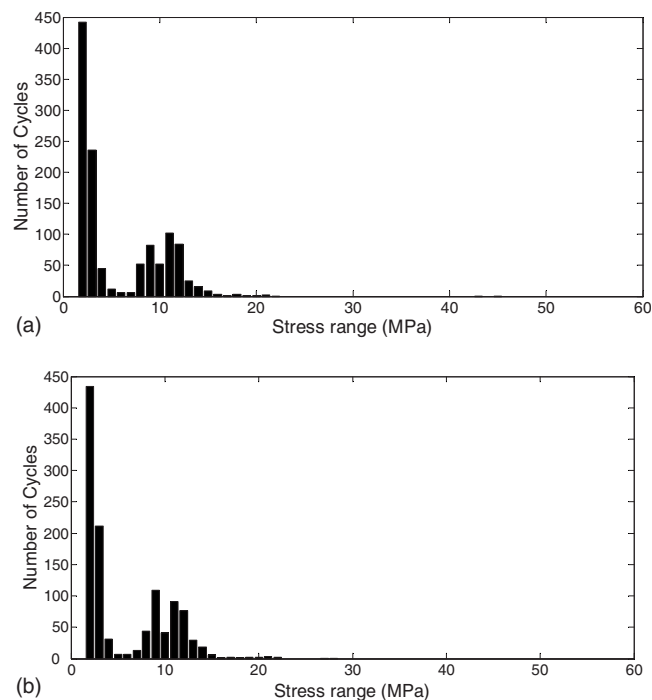**Fig. 4.** Histograms of daily stress spectra: (a) September 23, 1999; (b) November 6, 1999

the peaks and valleys in the stress time history, daily stress spectra are procured by the rainflow counting algorithm (Downing and Socie 1982). Fig. 4 shows the histograms of two typical daily stress spectra by specifying a resolution of 1 MPa for the stress range interval. The stress cycles with amplitudes less than 2 MPa are discarded because the lower valid limit of the strain gauge is 10 microstrains.

Fig. 4 reveals that the daily stress spectra are similar for different days experiencing normal traffic and wind conditions. It is therefore reasonable to average a number of daily stress spectra resulting from different days to obtain an average standard daily stress spectrum. Furthermore, in recognizing that the strain time history due to typhoon has a pattern different from that under normal traffic and wind conditions (Ye et al. 2007b), the stress spectrum under typhoon conditions should be taken into account in derivation of the standard stress spectrum. According to the record from the Hong Kong Observatory, there are a total of 22 out of 365 days (one year), which were under typhoon conditions in 1999. According to the investigation by Ye et al. (2007a), it is appropriate to assess the fatigue life for the Tsing Ma Bridge by using 20 daily strain data to obtain an average standard daily stress spectrum. As a result, data acquired from 20 days including one day under typhoon conditions are chosen to construct a representative data sample. Fig. 5 illustrates the obtained standard daily stress spectrum using the 20 days' daily stress spectra in consideration of highway traffic, railway traffic, and typhoon effects.

### *Joint PDF of Hot Spot Stress Range*

Multimodal PDF of Stress Range
The rainflow-counted stress ranges from 2 to 30 MPa are extracted for modeling the PDF of the stress range measured by the strain gauge SPTLS16, as this scope covers all the stress ranges caused by the vehicle and train traffic passing through the bridge.

The total observation number of the 20-day stress range data are 30,986 and the number of classes is obtained as 16 according to the Sturges classification rule (Sturges 1926). Figs. 6 and 7 show the finite mixed PDFs and CDFs of the 20-days stress range data acquired by the strain gauge SPTLS16 when using normal, lognormal, and Weibull distributions, respectively. The corresponding estimated parameters of the component distributions are given in Table 1. It can be seen that the scatter of the stress ranges is well modeled by the finite mixture distributions and easily extrapolated to the region beyond the measured stress ranges. The accuracy of the stress range prediction and the extrapolation ability rely on the probability distribution of the stress range. In addition, the scattered level and the record length of the stress range will also affect the accuracy when extrapolating beyond the measured stress ranges (Nagode and Fajdiga 1998). It is observed in Fig. 6 that the predicted stress range distribution is a two-modal PDF separated at 6 MPa. The stress ranges less than 6 MPa are caused by highway traffic, and the stress ranges larger than 6 MPa are mainly attributed to train traffic.
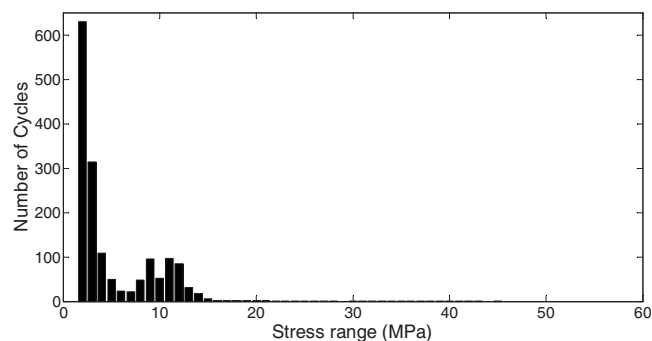
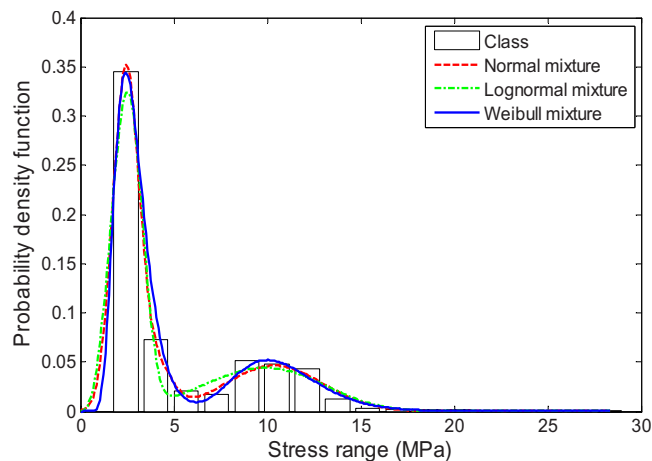**Fig. 5.** Histogram of standard daily stress spectrum

Fig. 6. Mixed PDFs of 20-day stress range data

Table 1. Estimated Parameters of Component Distributions from 20-Day Stress Range Data

Parametric family	Weight (w)	Mean value (μ)	Standard deviation (σ)
Normal	0.603	2.428	0.698
	0.304	10.373	2.611
	0.093	4.046	0.842
Lognormal	0.711	0.991	0.322
	0.289	2.351	0.216
Weibull		Shape parameter (θ)	Shape parameter (γ)
	0.651	2.751	3.537
	0.349	10.854	3.584

Fig. 8 shows the variation of the AIC values with the iteration number of the three mixed PDFs (normal, lognormal, and Weibull) of the 20-day stress range data. The best model of the stress range distribution is determined with the lowest AIC value. It is found that the AIC values for the three PDFs converge rapidly and the mixed Weibull PDF results in the lowest AIC value. As a result, the Weibull distribution is taken herein as the component distribution for modeling the measured stress ranges. The AIC value helps the selection of both the optimal number of components and the parametric family.

Numerical Analysis of SCF

A three-dimensional global FEM of Tsing Ma Bridge is established using the general-purpose commercial software ABAQUS as illustrated in Fig. 9. The beam and shell elements in the ABAQUS element library are chosen to model the structural components of the bridge. There are 7,375 nodes and 17,677 elements in the global FEM. After verifying the predicted responses (dynamic modal properties and displacement/strain influence lines) of the global FEM by field measurement data (Wang et al. 2000; Wong 2005), a three-dimensional local FEM of typical welded connections extracted from the section CH24662.5 where the strain gauge SPTLS16 is attached under the track plate of the railway beam, is formulated as shown in Fig. 10. There are
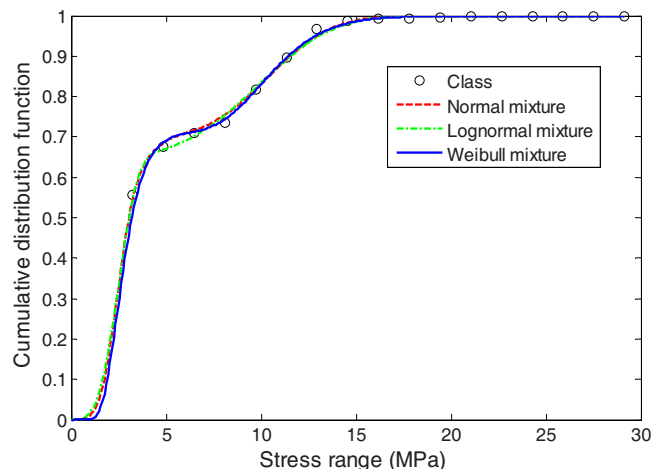
502,879 nodes and 406,448 elements in this local FEM, and the displacement responses at the deck cross sections obtained from the global FEM are adopted as boundary conditions of the local FEM.

The dimension of the typical welded joint in the local FEM is identical to the drawing details of Tsing Ma Bridge. The weld is simply modeled as a triangle and the weld thickness and weld angle are 6 mm and 45°, respectively. A relatively fine grid mesh is used for the weld seam where stress concentration with a high stress gradient is expected, and a coarse grid mesh is used for the zone where stresses are relatively uniform. As a compromise between the mesh size and number of degrees of freedom, the eight-node reduced integration continuum element is adopted in modeling the plate and weld.

Fig. 11 illustrates the weld stress analysis of the welded joint at the strain gauge SPTLS16. It reveals that the hot spot near the strain gauge SPTLS16 is located at the end of the longitudinal weld which is serving as the linkage between the railway beam web and the track plate. A uniformly distributed load of 1 MPa is applied on the rail-track areas of the track plate in the local FEM, and then the nominal stress at the location of the strain gauge SPTLS16 and the structural stress at the hot spot are obtained. Finally, the SCF for the welded joint monitored by the strain gauge SPTLS16 is determined as 1.379 according to Eq. (17).

PDF of Hot Spot Stress Range

The joint PDF of hot spot stress range can be obtained by Eq. (5) when the PDFs of stress range and SCF have been determined.
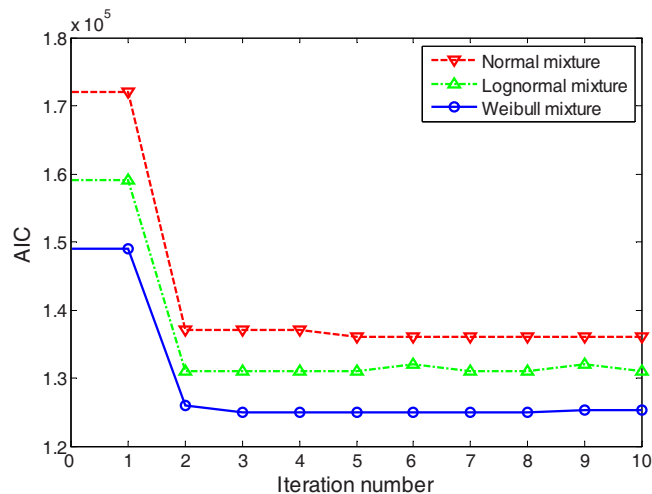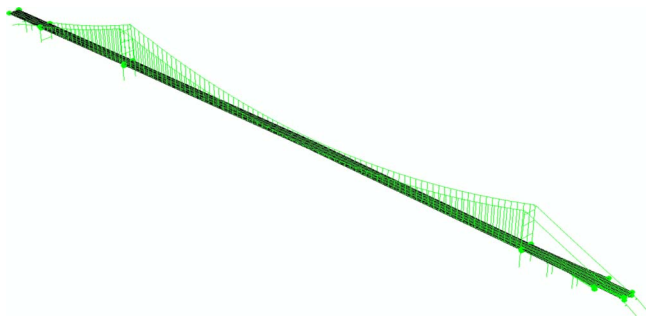

Fig. 7. Mixed CDFs of 20-day stress range data

Fig. 8. AIC values of mixed PDFs of 20-day stress range data

Fig. 9. Three-dimensional global FEM of Tsing Ma Bridge

Fig. 11. Weld stress analysis of welded joint at strain gauge SPTLS16

For the welded detail in concern, the SCF is found by full-scale model experiments to conform to the normal distribution with a coefficient of variation (COV) of 0.021 (Ye 2010). As a result, the PDF of the SCF is formulated by a normal distribution with a mean value of 1.379 and a COV of 0.021 as shown in Fig. 12. The joint PDF of hot spot stress range is subsequently obtained from the multimodal PDF of stress range and the PDF of SCF, as illustrated in Fig. 13.

Probabilistic Assessment of Fatigue Life

The double-tier deck of Tsing Ma Bridge is a redundant structural system. In the present study, the fatigue life of this bridge is evaluated only in a component level. An accurate assessment of the fatigue life and reliability of the entire bridge should be conducted by making use of the theory and methodology of system reliability (Zhao and Ang 2003; Imai and Frangopol 2002). This requires further research beyond the scope of this paper. In this study, the detail category at the hot spot location and relevant parameters in the proposed fatigue reliability model are determined based on BS5400 Part 10 [British Standards Institution (BSI) 1980], which is adopted as a design standard for Tsing Ma Bridge. According to BS5400 Part 10, the type of detail at the location of the strain gauge SPTLS16 is categorized into the class F2, and thus the values of the parameters m and C are determined as $m=3.0$ and $C=0.43 \times 10^{12}$. For various detail classes, the relevant values of these parameters are different and detailed in BS5400 Part 10. In general, fatigue failure of a structural component is assumed to happen when the final summation of the elementary damage reaches a predetermined value known as fatigue damage index. The fatigue life of the welded detail monitored by the strain gauge SPTLS16 is predicted to be 716 years when the damage index equals to unity as a deterministic value. While the predicted fatigue life is 927 years when using the method illustrated in Byers et al. (1997a), in which only the prob-
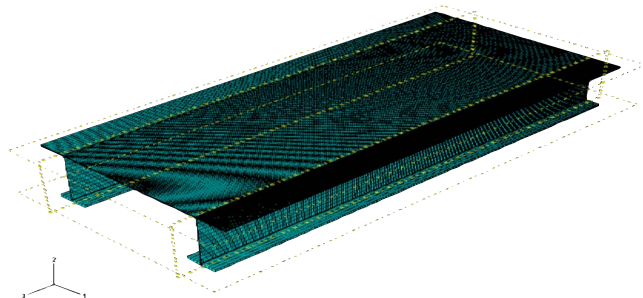
ability distribution of the nominal stress range is accounted for in the fatigue reliability model. It indicates that the predicted fatigue life is reduced by 23% when taking the stress concentration into consideration.

Traffic volume is an important parameter in fatigue life assessment of bridge structures. With the growth of the traffic volume, the number of cycles of stress ranges will be increased resulting in the growth of fatigue damage as well as the reduction of the fatigue life of bridge components (Mohammadi et al. 1998). The Tsing Ma Bridge was opened in April 1997 to carry both railway and highway traffic. The railway traffic is regular and would not grow noticeably. However, the highway traffic volume is steadily increasing over years. According to the Annual Traffic Census performed by the Traffic and Transport Survey Division of the Transport Department of Hong Kong SAR Government [Traffic and Transport Survey Division of the Transport Department (TTSD) of Hong Kong SAR Government 2004], the traffic volume growth of Tsing Ma Bridge in 1999 was 44.6%. Such a great rise in traffic volume is due to the opening of the new Hong Kong International Airport in July 1998. The traffic volume growth of the bridge becomes steady with a 1.85% annual growth rate after the year of 2000. Taking the growth of traffic volume into consideration, the estimated fatigue life at the welded detail concerned in this study is 249 years, which is significantly reduced in comparison with that without considering traffic growth. In reality, however, the carrying capacity of the bridge is restricted and the traffic volume would not increase infinitely. Assuming the
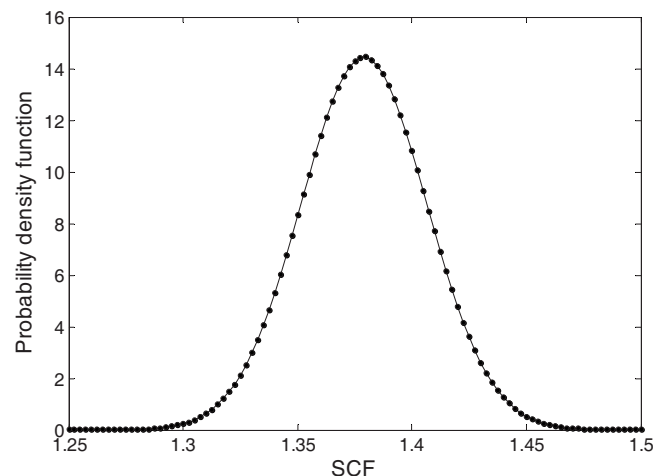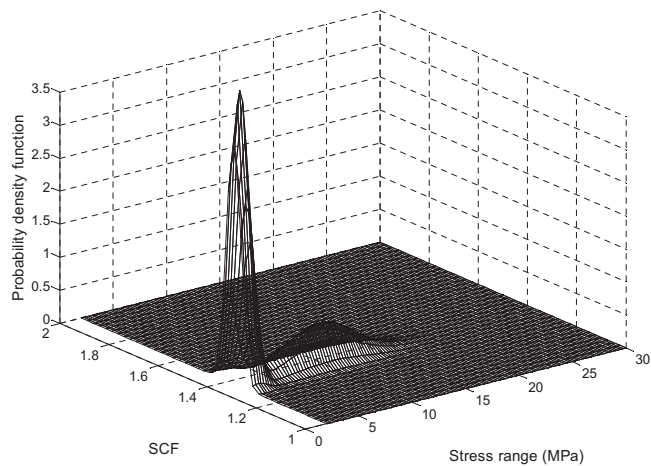

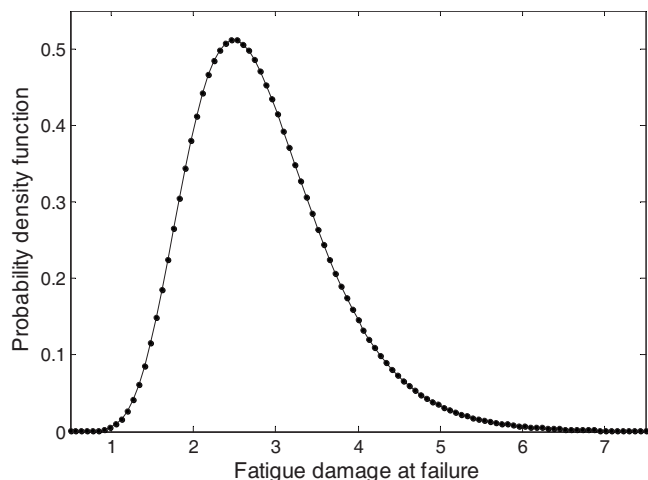**Fig. 10.** Three-dimensional local FEM of welded connections

Fig. 12. PDF of the SCF

Fig. 13. Joint PDF of hot spot stress range

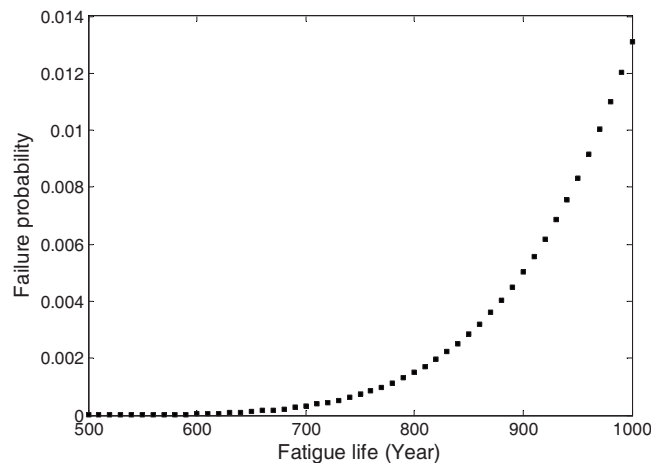**Fig. 15.** Failure probability versus fatigue life

highway traffic volume tends to be stable until 2027 for instance, the predicted fatigue life is 692 years in comparison with the design fatigue life of 500 years for this bridge (Wong 2007).

In fact, the fatigue damage at failure is a random variable which may be modeled by a lognormal distribution with a mean value of 1 and a COV of 0.3 (Wirsching and Chen 1988). The PDF of the fatigue damage at failure is shown in Fig. 14. By applying the method developed in this study, the failure probability and reliability index versus fatigue life are obtained as shown in Figs. 15 and 16, where the range of the counted stress is between 2 and 30 MPa and the coverage of SCF is from 1 to 2. It is seen that fatigue life can be determined for a given target reliability index or failure probability. In the present study, the predicted fatigue life is related to the structural component failure rather than to the entire bridge failure in a system level. This leads to the predicted fatigue life relatively high and the probability of failure relatively low. Another reason for this concern is because most of the measured stress ranges are lower than the fatigue limit which is 35 MPa for the detail category in this study [British Standards Institution (BSI) 1980].

A target reliability index is defined as the value of reliability index that is acceptable for design or evaluation, and its selection should be based on economic considerations as well, involving cost of construction, inspection, repair, rehabilitation, and re-

placement. The reliability index in the range between 2 and 4 has been used in establishing code safety margins (AISC 1986) and the value of target reliability index recommended for offshore structural components is 3 (Wirsching and Chen 1987). From Fig. 16, the reliability index is estimated to be approximately 4.5 in accordance with the design fatigue life of 500 years for this bridge. Figs. 15 and 16 also indicate that the service fatigue life directly affects the probability of failure or reliability index of the structural component. When the service life requirement is increased, the corresponding reliability index decreases sharply.

Conclusions

In this study, a fatigue reliability model has been proposed by uniquely integrating the probability distribution of hot spot stress range with a continuous probabilistic formulation of Miner's rule, and has been applied for probabilistic fatigue life assessment of Tsing Ma Bridge by use of the strain monitoring data from a long-term SHM system which has been permanently installed on the bridge. Considering highway and railway traffic and typhoon effects, a monitoring-based standard stress spectrum was achieved by carefully examining one-year strain measurement data. The method of finite mixture distributions in conjunction with a hy-

Fig. 14. PDF of the fatigue damage at failure
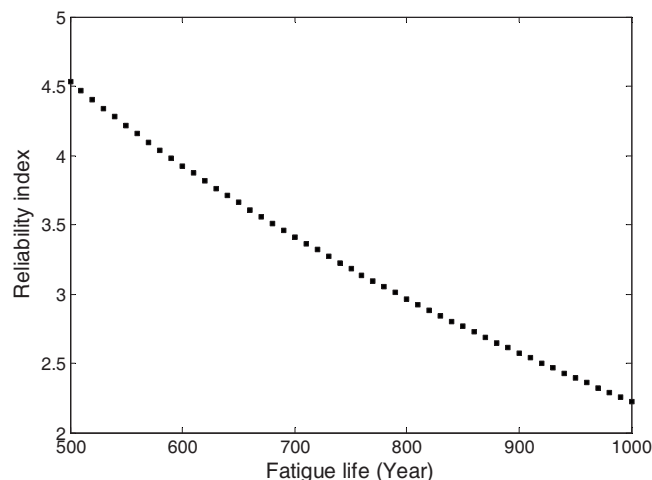
Fig. 16. Reliability index versus fatigue life

brid parameter estimation approach was applied to generate the PDF of stress range, while SCFs at fatigue-critical locations were calculated by finite-element analysis method. The joint PDF of hot spot stress range and subsequently the failure probability and reliability index versus fatigue life were obtained by structural reliability theory. The results show that: (1) the measured stress distribution with multimodal properties can be accurately represented in an explicit expression by the method of finite mixture distributions in conjunction with a hybrid parameter estimation approach; (2) the service fatigue life significantly affects the probability of failure or reliability index of the welded detail in study, and the reliability index decreases sharply when the service life requirement is increased; and (3) the proposed approach provides a viable way for conducting monitoring-based fatigue reliability assessment of steel bridges taking account for uncertainty and randomness inherent in the fatigue phenomenon and measurement data.

Acknowledgments

References

AISC. (1986). *Load and resistance factor design specifications for structural steel buildings*, American Institute of Steel Construction, Chicago.

Akaike, H. (1974). "A new look at the statistical model identification." *IEEE Trans. Autom. Control*, 19(6), 716–723.

Albrecht, P., and Lenwari, A. (2009). "Variable-amplitude fatigue strength of structural steel bridge details: Review and simplified model." *J. Bridge Eng.*, 14(4), 226–237.

American Welding Society (AWS). (1998). "Structural welding code-steel." *ANSI/AWS D1.1-98*, Miami.

Basquin, O. H. (1910). "Exponential law of endurance tests." *Proc., ASTM*, Vol. 10, ASTM, West Conshohocken, Pa., 625–630.

British Standards Institution (BSI). (1980). "Steel, concrete and composite bridges. Part 10: Code of practice for fatigue." *BS5400*, London.

Brownjohn, J. M. W. (2007). "Structural health monitoring of civil infrastructure." *Philos. Trans. R. Soc. London, Ser. A*, 365(1851), 589–622.

Byers, W. G., Marley, M. J., Mohammadi, J., Nielsen, R. J., and Sarkani, S. (1997a). "Fatigue reliability reassessment procedures: State-of-the-art paper." *J. Struct. Eng.*, 123(3), 271–276.

Byers, W. G., Marley, M. J., Mohammadi, J., Nielsen, R. J., and Sarkani, S. (1997b). "Fatigue reliability reassessment applications: State-of-the-art paper." *J. Struct. Eng.*, 123(3), 277–285.

Chan, T. H. T., Zhou, T. Q., Li, Z. X., and Guo, L. (2005). "Hot spot stress approach for Tsing Ma Bridge fatigue evaluation under traffic using finite element method." *Struct. Eng. Mech.*, 19(3), 261–279.

Chiew, S. P., Lie, S. T., Lee, C. K., and Huang, Z. W. (2004). "Fatigue performance of cracked tubular T joints under combined loads. I: Experimental." *J. Struct. Eng.*, 130(4), 562–571.

Cho, H. N., Lim, J. K., and Choi, H. H. (2001). "Reliability-based fatigue failure analysis for causes assessment of a collapsed steel truss bridge." *Eng. Failure Anal.*, 8(4), 311–324.

Connor, R. J., and Fisher, J. W. (2006). "Consistent approach to calculating stresses for fatigue design of welded rib-to-web connections in steel orthotropic bridge decks." *J. Bridge Eng.*, 11(5), 517–525.

Crespo-Minguillon, C., and Casas, J. R. (1998). "Fatigue reliability analysis of prestressed concrete bridges." *J. Struct. Eng.*, 124(12), 1458–1466.

DeWolf, J. T., Lauzon, R. G., and Culmo, M. P. (2002). "Monitoring bridge performance." *Struct. Health Monit.*, 1(2), 129–138.

Doerk, O., Fricke, W., and Weissenborn, C. (2003). "Comparison of different calculation methods for structural stresses at welded joints." *Int. J. Fatigue*, 25(5), 359–369.

Downing, S. D., and Socie, D. F. (1982). "Simple rainflow counting algorithms." *Int. J. Fatigue*, 4(1), 31–40.

Duda, R. O., and Hart, P. E. (1973). *Pattern classification and scene analysis*, Wiley, New York.

European Committee for Standardization (CEN). (1992). "Design of steel structures, part 1.1." *Eurocode 3*, Brussels, Belgium.

Fisher, J. W. (1984). *Fatigue and fracture in steel bridges: Case studies*, Wiley, New York.

Gandhi, P., and Berge, S. (1998). "Fatigue behavior of T-joints: Square chords and circular braces." *J. Struct. Eng.*, 124(4), 399–404.

Gurney, T. R. (1979). *Fatigue of welded structures*, 2nd Ed., Cambridge University Press, Cambridge, England.

Imai, K., and Frangopol, D. M. (2002). "System reliability of suspension bridges." *Struct. Safety*, 24(2–4), 219–259.

International Institute of Welding (IIW). (2000). "Fatigue design procedures for welded hollow section joints." *IIW Doc. XIII-1804-99/XV-1035-99. Recommendations for IIW subcommision XV-E*, Abington Publishing, Cambridge, England.

Kim, S. H., Lee, S. W., and Mha, H. S. (2001). "Fatigue reliability assessment of an existing steel railroad bridge." *Eng. Struct.*, 23(10), 1203–1211.

Ko, J. M., and Ni, Y. Q. (2005). "Technology developments in structural health monitoring of large-scale bridges." *Eng. Struct.*, 27(12), 1715–1725.

Lie, S. T., Chiew, S. P., Lee, C. K., and Huang, Z. W. (2004). "Fatigue performance of cracked tubular T joints under combined loads. II: Numerical." *J. Struct. Eng.*, 130(4), 572–581.

McLachlan, G. J., and Peel, D. (2000). *Finite mixture models*, Wiley, New York.

Miner, M. A. (1945). "Cumulative damage in fatigue." *J. Appl. Mech.* 12(3), 159–164.

Mohammadi, J. (2001). "Input data requirements for fatigue reliability analysis of aging structures." *Proc., Structures Congress and Exposition 2001* (CD-ROM), P. C. Chang, ed., ASCE, Reston, Va.

Mohammadi, J., Guralnick, S. A., and Polepeddi, R. (1998). "Bridge fatigue life estimation from field data." *Pract. Period. Struct. Des. Constr.*, 3(3), 128–133.

Morgan, M. R., and Lee, M. M. K. (1998a). "Parametric equations for distributions of stress concentration factors in tubular K-joints under out-of-plane moment loading." *Int. J. Fatigue*, 20(6), 449–461.

Morgan, M. R., and Lee, M. M. K. (1998b). "Stress concentration factors in tubular K-joints under in-plane moment loading." *J. Struct. Eng.*, 124(4), 382–390.

Moses, F., Schilling, C. G., and Raju, K. S. (1987). "Fatigue evaluation procedures for steel bridges." *NCHRP Rep. No. 299*, Transportation Research Board, Washington, D.C.

Nagode, M., and Fajdiga, M. (1998). "On a new method for prediction of the scatter of loading spectra." *Int. J. Fatigue*, 20(4), 271–277.

Nagode, M., and Fajdiga, M. (2006). "An alternative perspective on the mixture estimation problem." *Reliab. Eng. Syst. Saf.*, 91(4), 388–397.

Ni, Y. Q., Ye, X. W., and Ko, J. M. (2006). "Fatigue reliability analysis of a suspension bridge using long-term monitoring data." *Key Eng. Mater.*, 321–323, 223–229.

Niemi, E., Fricke, W., and Maddox, S. J. (2006). *Fatigue analysis of welded components: Designer's guide to the structural hot-spot stress approach*, CRC, Boca Raton, Fla.

Pines, D. J., and Aktan, A. E. (2002). "Status of structural health moni-

toring of long-span bridges in the United States." *Prog. Struct. Eng. Mater.*, 4(4), 372–380.

Pourzeynali, S., and Datta, T. K. (2005). "Reliability analysis of suspension bridges against fatigue failure from the gusting of wind." *J. Bridge Eng.*, 10(3), 262–271.

Poutiainen, I., Tanskanen, P., and Marquis, G. (2004). "Finite element methods for structural hot spot stress determination—A comparison of procedures." *Int. J. Fatigue*, 26(11), 1147–1157.

Reed, R. P., Smith, J. H., and Christ, B. W. (1983). "The economic effects of fracture in the United States." *Special publication 647-1*, National Bureau of Standards, U.S. Department of Commerce, Washington, D.C.

Schijve, J. (2001). *Fatigue of structures and materials*, Kluwer, Dordrecht, The Netherlands.

Schilling, C. G., Klippstein, K. H., Barson, J. M., and Blake, G. T. (1978). "Fatigue of welded steel bridge members under variable-amplitude loadings." *NCHRP Rep. No. 188*, Transportation Research Board, Washington, D.C.

Steiner, P. M., and Hudec, M. (2007). "Classification of large data sets with mixture models via sufficient EM." *Computational Statistics & Data Analysis*, 51(11), 5416–5428.

Stephens, R. I, Fatemi, A., Stephens, R. R., and Fuchs, H. O. (2001). *Metal fatigue in engineering*, 2nd Ed., Wiley, New York.

Sturges, H. A. (1926). "The choice of a class interval." *J. Am. Stat. Assoc.*, 21(153), 65–66.

Szerszen, M. M., Nowak, A. S., and Laman, J. A. (1999). "Fatigue reliability of steel bridges." *J. Constr. Steel Res.*, 52(1), 83–92.

Titterington, D., Smith, A., and Makov, U. (1985). *Statistical analysis of finite mixture distributions*, Wiley, New York.

Traffic and Transport Survey Division of the Transport Department (TTSD) of Hong Kong SAR Government. (2004). *The Annual Traffic Census 2003, Publication No. 04CAB1*, Hong Kong.

Wang, J. Y., Ko, J. M., and Ni, Y. Q. (2000). "Participation of local modes in seismic response of Tsing Ma Suspension Bridge." *Advances in structural dynamics*, Vol. 2, J. M. Ko and Y. L. Xu, eds., Elsevier Science, Oxford, U.K., 963–970.

Wirsching, P. H., and Chen, Y. N. (1987). "Fatigue design criteria for TLP tendons." *J. Struct. Eng.*, 113(7), 1398–1414.

Wirsching, P. H., and Chen, Y. N. (1988). "Considerations of probability-based fatigue design for marine structures." *Mar. Struct.*, 1(1), 23–45.

Wong, K. Y. (2004). "Instrumentation and health monitoring of cable-supported bridges." *Struct. Control Health Monit.*, 11(2), 91–124.

Wong, K. Y. (2007). "Structural health monitoring of Tsing Ma Bridge." *Proc., 5th Workshop on Nondestructive Evaluation of Civil Infrastructural System*, Society of Nondestructive Testing, Taipei, Taiwan, 33–56.

Wong, K. Y., and Ni, Y. Q. (2009). "Modular architecture of structural health monitoring system for cable-supported bridges." *Encyclopedia of structural health monitoring*, C. Boller, F.-K. Chang, and Y. Fujino, eds., Vol. 5, Wiley, Chichester, U.K., 2089–2105.

Wong, M. P. (2005). "Validation of Tsing Ma Bridge influence coefficients using measurement data." *Project Rep. Prepared for Dept. of Civil and Structural Engineering*, The Hong Kong Polytechnic Univ., Kowloon, Hong Kong.

Ye, X. W. (2010). "Fatigue reliability assessment of steel bridges instrumented with structural health monitoring system." Ph.D. thesis, Dept. of Civil and Structural Engineering, The Hong Kong Polytechnic Univ., Kowloon, Hong Kong.

Ye, X. W., Ni, Y. Q., and Ko, J. M. (2007a). "Hot spot stress approach for fatigue life assessment in welded bridge connections using monitoring data and FEM analysis." *Proc., 3rd Int. Conf. on Structural Health Monitoring and Intelligent Infrastructure* (CD-ROM), Vancouver, Canada.

Ye, X. W., Ni, Y. Q., and Ko, J. M. (2007b). "Monitoring-based fatigue life assessment of a suspension bridge accounting for both traffic and typhoon effects." *Proc., 4th Cross-Strait Conf. on Structural and Geotechnical Engineering*, Zhejiang University Press, Hangzhou, China, 832–843.

Zhao, Y. G., and Ang, A. H. S. (2003). "System reliability assessment by method of moments." *J. Struct. Eng.*, 129(10), 1341–1349.